Geotechnical Aspects of Underground Construction in Soft Ground – Viggiani (ed)
© 2012 Taylor & Francis Group, London, ISBN 978-0-415-68367-8

Tunneling in stratified soft ground: Experimental study on 1g EPBS reduced scale model

N. Berthoz, D. Branque, H. Wong & G. Généreux
Université de Lyon, Ecole Nationale des Travaux Publics de l'Etat, Département Génie civil et Bâtiment, FRE CNRS 3237, Vaulx-en-Velin, France

D. Subrin & E. Humbert
Centre d'Etudes des Tunnels, Avenue François Mitterrand, Bron cedex, France

ABSTRACT: This paper presents several results concerning soft ground tunneling with Earth Pressure Balanced Shield (EPBS), obtained on reduced scale model. Under the condition of "equilibrium rate tunneling", surface settlements and arching effects around the TBM are analyzed in homogeneous and stratified soils, with a particular attention on the influences of face pressure and soil mass configuration. Failure mechanisms by face collapse, observed in homogeneous pure frictional and frictional-cohesive materials as well as stratified soils (cases of two and three-layered soils), are then presented.

1 INTRODUCTION

Estimation of critical tunnel face pressures required in low resistance soils as well as forecasting surface settlements for pressurized shield tunneling has been the subject of different experimental works using 1g or centrifuged physical laboratory models (Meguid & al, 2008). Note that most of these studies were conducted on homogeneous soils.

However, stratified soil layers with different mechanical properties are frequently encountered in practice (Chu & al, 2007). To date, only a few studies using centrifuged reduced scale model and with "pressurized air bags" were reported on stratified soils (Hagiwara & al, 1999; Caporaletti & al, 2008).

The "Département Génie Civil et Bâtiment" of ENTPE has developed an original reduced scale model of EPBS. It is able to recreate, under normal gravity, the different phases of excavation process. The objective is to analyze in order to better understand the mechanisms involved for this excavation method, to provide assistance to steering on site, to develop theoretical and numerical tools of tunnel design. Different tests, firstly performed on homogeneous pure frictional (Branque & al, 2002) and frictional-cohesive materials (Doan, 2007), are then extended to stratified soils so as to get closer to the prevailing conditions on site.

This paper presents the main results obtained for these materials. Regarding the equilibrium rate tunneling (rate minimizing ground deformations), the influences of face pressure and soil mass configuration on surface settlements and arching effects around the TBM are studied. Failure mechanisms by face collapse, exhibited on reduced scale model in two and three-layered soils, are then analyzed and compared to those observed in homogeneous soils.

2 THE ENTPE EPBS MODEL

2.1 *Description of the experimental setup*

The ENTPE EPBS model (geometric scale between 1/4 and 1/20) allows to reproduce the main features of this excavation method: excavation of soil by the cutter head (diameter: 0,55 m), face confinement by excavated material contained in the working chamber, immediate radial confinement by the cylindrical steel shield tail (Cf. Figure 1). Note that an uniform surcharge q may be applied on ground surface by means of air chambers.

The EPBS model features an extensive instrumentation very similar to real TBM's: measures of the torques on the cutting wheel and screw conveyor, the axial thrust exerted by the cylinder, the pressures in the working chamber, the mass of material discharged and the shield penetration speed. It also offers the ability to monitor extensively the soil mass with surface and internal displacement sensors (type LVDT) and internal total stress sensors (Entran EPN50 and Kyowa BE2KC).

During the tests, the TBM penetrates into the ground through a circular hole on the container wall. Maximum penetration is 1m. Tests are composed of two phases: an equilibrium rate tunneling is carried out during the first 95 centimeters of excavation,

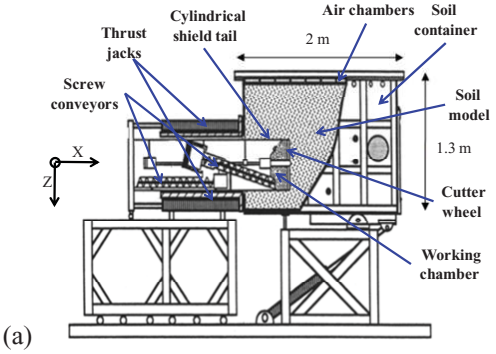

(a)

(b)

Figure 1. Sectional diagram (a) and photography (b) of EPBS model of ENTPE.

followed by an over-extraction (under-extraction) period, source of a lack (excess) of confinement of the working face, and leading the soil mass to failure.

2.2 *Soil models and configurations studied*

Soil mass models are prepared from Hostun S28 dry sand (purely frictional) or slightly wet (frictional-cohesive). For this second case, the cohesion depends on water content and density of the sand.

Soil models and the mode of preparation (poured at zero height for purely frictional material and layer-by-layer compaction for frictional cohesive material) have been identified taking into account the similitude conditions (partial similitude defined by Mandel (1962) and described in Doan (2007)).

Due to the low level of stresses prevailing in the reduced scale model, soil mass is prepared in a loose state so as to approach the ideal similitude on the volumetric behavior (Scott, 1989). Density and water content are controlled during soil mass confection.

Two types of stratification were analyzed (Figure 2): two-layered soil (self-stable frictional cohesive layer just underneath the tunnel axis and purely frictional above) and three-layered soil (same configuration as for the two-layered soil but with an additional layer of frictional-cohesive soil at the limit of stability above the crown).

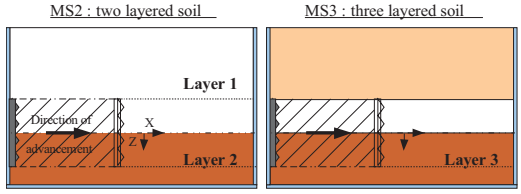

Figure 2. Longitudinal section of stratified soils.

Table 1. Mechanical characteristics of soils models.

Test	γ (kN/m³)	Dr (%)	E_t (MPa)	c′ (kPa)	φ′ (°)	ψ′ (°)	q (kPa)
MC3	13.20	0.7	10	2.5	36	5	0
MC4	13.15	0.7	10	1.5	36	5	0
MC5	13.05	0.6	10	0.5	36	5	0
MC6	13.05	0.6	10	0.5	36	5	50
MC7	13.05	0.6	10	0.5	36	5	50
MC8	13.05	0.6	10	0.5	36	5	0
MF11	13.70	0.2	5	0	39	2	0
MF13	13.70	0.2	5	0	39	2	0
MS2 1	13.25	0.0	5	0	39	2	0
2	13.30	0.7	10	3	36	5	0
MS3 1	13.20	0.7	10	0.5	36	5	0
2	13.25	0.0	5	0	39	2	0
3	13.30	0.7	10	3	36	5	0

Mechanical characteristics (total weight γ, relative density Dr, apparent cohesion c′, friction angle φ′ and dilatancy angle ψ′) of different homogeneous and stratified soil masses studied in this paper are given in Table 1. These mechanical characteristics have been obtained with triaxial, trench stability and Casagrande shear tests.

3 SURFACE SETTLEMENTS

Under equilibrium rate tunneling, the vertical displacements measured at the ground surface reveal a stationary behavior. Hence, the longitudinal settlement profiles relative to the reference frame attached to the shield is independent of the position of the latter (Berthoz & al, 2010).

Figure 3 summarizes for all tests carried out under ideal tunneling rate the contours of longitudinal settlement profiles. These are inferred from stationary behavior described above.

Note firstly that only 30 to 60% of settlement measured at 1D at the rear of the working face are observed before passage of the shield and may be related to volume losses occurring at the front (compressive action of the cutting wheel, lack of front pressure…), the remainder being generated behind the face by shearing along the cylindrical shield tail (no overcut).

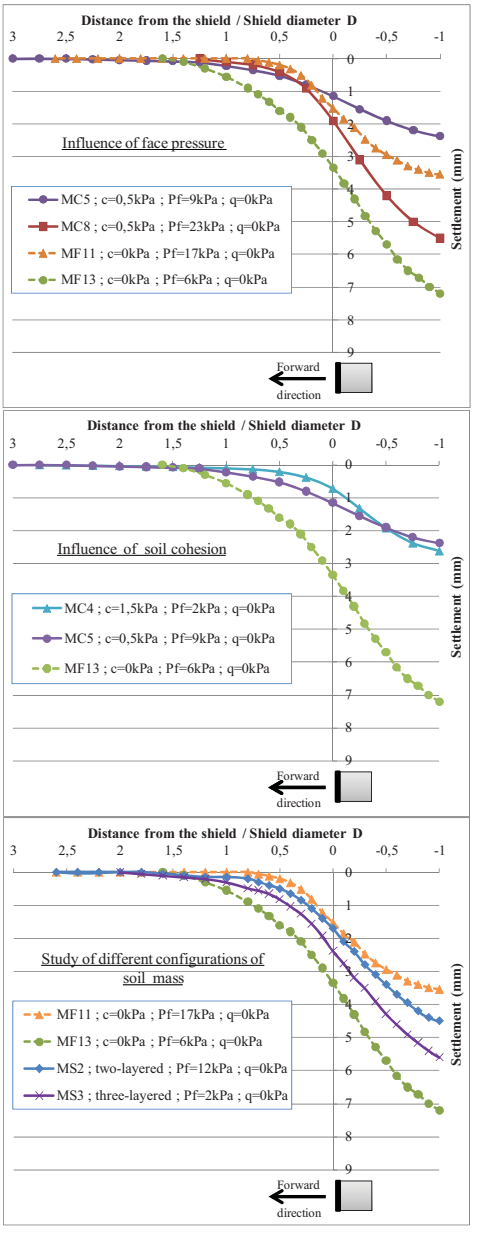

Figure 3. Contours of longitudinal settlements profiles inferred from stationary behavior in equilibrium rate tunneling.

Also, note that the magnitude of settlements observed on the reduced scale model (several mm) is consistent but relatively large compared to those that can be measured in situ (several cm), taking into account the scale ratio. Recall that our objective was to control them under different conditions.

Concerning influences of average face pressure (Pf) and soil cohesion on ground settlements, results of analyses show that the settlements generated in front of the working face decrease as the conditions of stability of the soil mass improve: increase of the face pressure or of the soil cohesion. It seems however that an important face pressure tends to amplify settlements behind the shield (test MC8 in relation to MC5). This result, consistent with those observed in extreme regime of under-extraction (Subrin & al, 2009), is explained by the appearance of horizontal tensile stresses in the ground above the shield.

In terms of stratified soils, the comparison between the results of tests MS2, MF11 and MF13 tends to show the lack of influence of the frictional-cohesive layer located underneath the tunnel axis. Given their regularity, it seems that the difference of the settlements observed during these three tests can be essentially attributed to the difference of the applied face pressures.. However, the stabilizing effect of a frictional-cohesive cover is undeniable as far as the settlements measured during test MS3 (three-layered soil) are of similar magnitudes as those observed in two-layered soil (test MS2) although face pressure was much lower.

4 LONGITUDINAL ARCHING EFFECT

Figure 4 shows the evolution of vertical stress measured along tunnel axis, at 0.2D above tunnel crown, during a phase of equilibrium rate tunneling. These measures reflect a stationary behavior characterized by a slight increase approaching the shield, followed by a strong decrease, even cancelling completely the vertical stress at the shield passage. Then it rises again to a value which can be sometimes higher than its initial value. This stress evolution during shield advancement explains by the existence of a longitudinal arching effect, already partially observed on a centrifuged model (Nomoto & al, 1999).

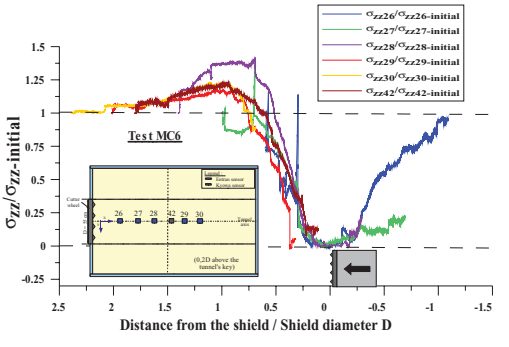

Figure 4. Stationary profile of stress measures 0.2D above the tunnel crown.

Figure 5 assembles contours of vertical stress profiles measured in the longitudinal direction, at 0.2D above the tunnel crown. These contours, deduced from the stationary behavior, show a slight shift (about 0.2D) of a lightened zone (due to arching effects) at the rear of the working face, indepedently of the tests conditions.

Moreover, in homogeneous purely frictional and frictional-cohesive grounds (figures 6a and 6b), a decrease of face pressure (relative to the initial horizontal stress at tunnel axis σ_{h0}) tends to generate higher displacements (Cf. paragraphs 3), thus mobilizing higher shear stresses, causing an enlargement of the lightened zone and a dicrease in the magnitude of load transfer to both sides of it.

Tests carried out also highlight the large increase of the extension of the lightened zone and the stronger decrease in the magnitude of load transferred to both sides of it, when soil cohesion increases. This observation, made for homogeneous soils, is in line with the increased ability to mobilize shear stresses with a higher cohesion.

This behavior is confirmed by tests performed in stratified soils. Indeed, case of three-layered soil (two-layered soil respectively), made with a frictional-cohesive overburden (purely frictional respectively) is similar to the frictional-cohesive (purely frictional respectively) homogeneous case.

5 FACE COLLAPSE

5.1 *Homogeneous soils*

In our tests, face collapse is obtained by a voluntary excessive discharge of the ground contained in the working chamber (over extraction rate). For frictional-cohesive materials, a failure mechanism in rigid blocks is observed, as evidence by the sudden nature of internal displacements measured close to the working face (Figure 6). Cutting the soil masses post-test showed that this failure block interfered with all the working face, and stretched up to 0.3D at the shield front and 0.1D above the crown, for tests performed with a cohesion of 0.5kPa (Figure 6 et Figure 8a). Note that this

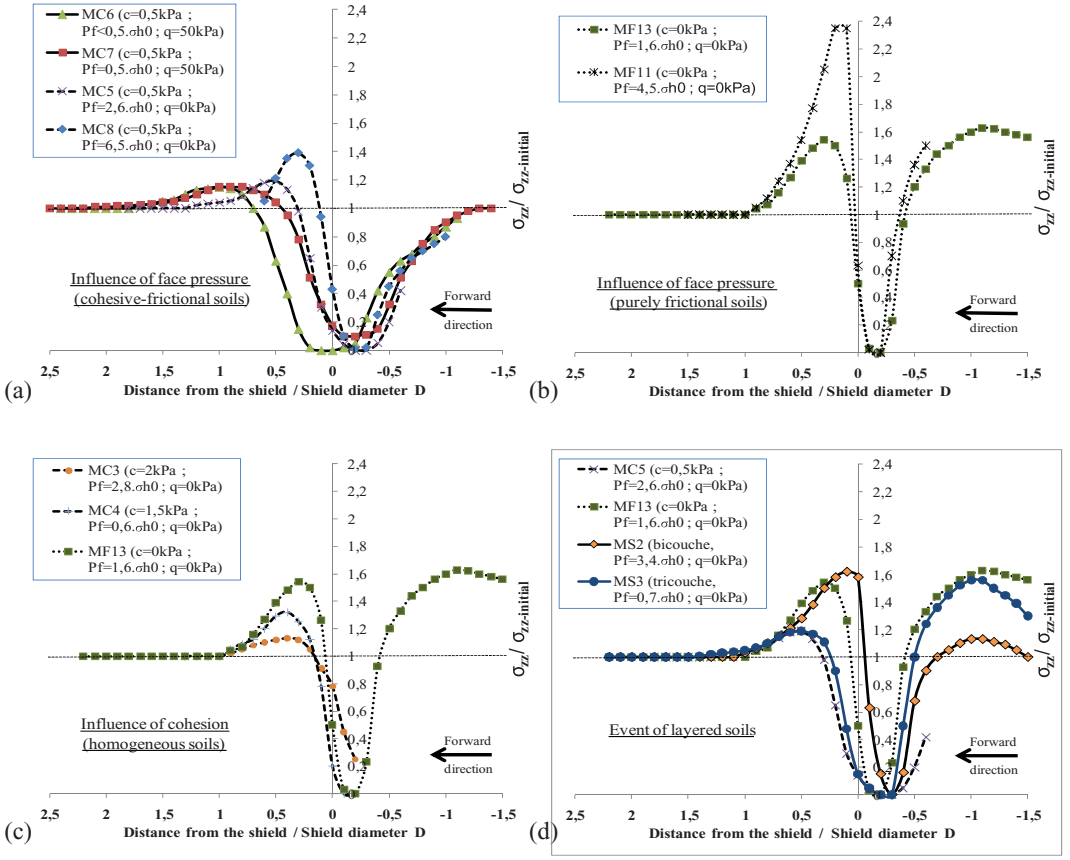

Figure 5. Contours of vertical stress profiles in equilibrium rate tunneling.

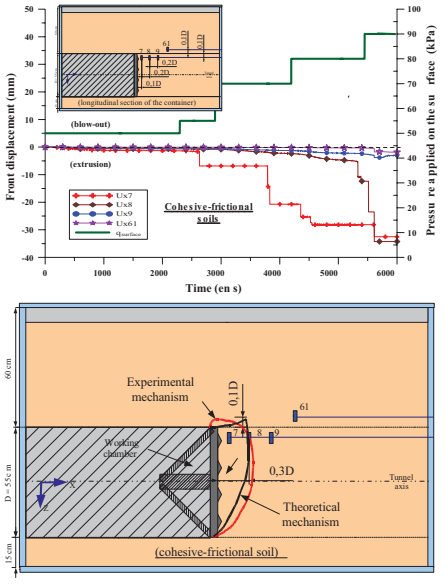

Figure 6. Main displacements and face collapse mechanism in homogeneous frictional-cohesive material.

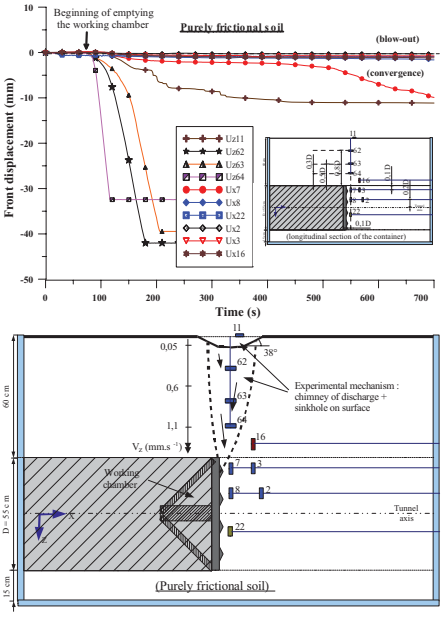

Figure 7. Main displacements and face collapse mechanism in homogeneous purely frictional material.

experimentally observed mechanism as well as the limit frontal pressures are in agreement with current theoretical approaches (Subrin & al, 2009).

In purely frictional soils, a chimney of discharge directly above the shield is observed. It is characterized by progressively increasing horizontal and vertical displacements (Figure 7) when the shield approaches. A circular sinkhole is generated at the ground surface (Figure 8b). Note that this flow originates near the crown and remains much localized as evidenced by the absence of displacements measured by frontal horizontal sensors. Note also that the vertical velocity of discharge decreases when approaching the surface, in accordance with the lateral extension of the void generated.

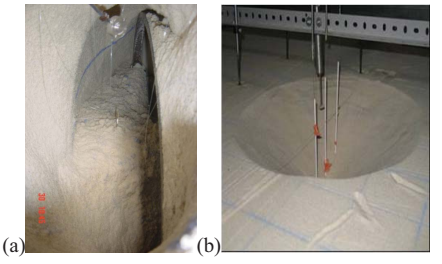

Figure 8. Photographs of face collapse mechanisms in frictional-cohesive (a) and purely frictional (b) soils.

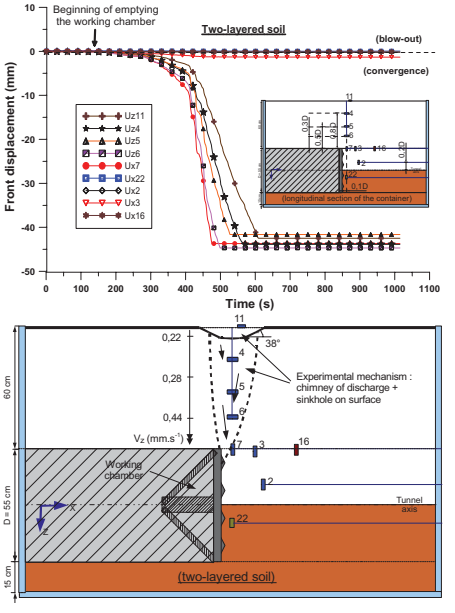

Figure 9. Main displacements and face collapse mechanism in two-layered soil.

5.2 *Stratified soils*

Failure mechanism observed in two-layered soil is very similar to that seen in homogeneous purely frictional soil, as evidenced by front displacements measured. The existence of cohesion or not underneath the tunnel axis does not alter significantly

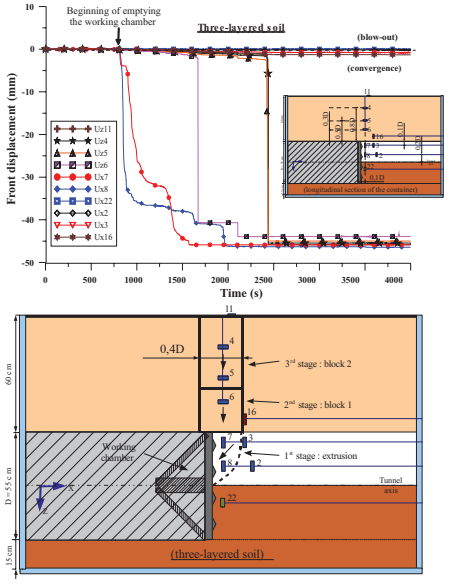

Figure 10. Main displacements and face collapse mechanism in three-layered soil.

the geometry of failure mechanism. However, it is interesting to note that vertical velocities v_z are lower in two-layered soil than in purely frictional soil, the rotation speed of screw conveyor being identical. The increase of cohesion of the material stirred in the working chamber thus limits strongly its ability to be extracted.

The test performed with a three-layered soil mass reveals an original face collapse mechanism, which is significantly different from homogeneous purely frictional and frictional-cohesive cases. This failure takes place in three phases as evidenced by displacement measurements (Figure 10). Firstly, flow of the purely frictional layer, located at the upper part of the working face, takes place, according to failure mechanisms commonly observed in these soils. The important decompression generated at the tunnel crown then causes a failure by blocks in the frictional-cohesive layer, the latter being at limiting stability. The last failure zone, a cylinder of diameter 0.4D off-centred at 0.1D front of the shield, is different from that observed in homogeneous frictional-cohesive soil, in accordance with the difference of loadings. Indeed, the flow occurring in purely frictional layer leads more to a "trap-door" type of loading than simply an insufficient face pressure.

6 CONCLUSION

Several results concerning tunneling in soft ground obtained from an EPBS reduced-scale physical model were presented in this paper.

For equilibrium-rate tunneling, influences of face pressure and soil mass configuration (value of cohesion, soil stratification) on surface settlements, tunnel crown displacements and longitudinal arching effects were analyzed.

Face collapse mechanisms in homogeneous purely frictional and frictional-cohesive soils were then described, followed by two mechanisms in stratified (two-layered and three-layered) soils. The first of these revealed the weak influence of a cohesive layer underneath the tunnel axis, except the ability to extract the material stirred in the working chamber. Finally, an original mechanism was exhibited in three-layered soils.

REFERENCES

Berthoz, N., Branque, D., Wong, H., & Subrin, D. 2010. Evolution des champs de contraintes et déplacements autour d'un tunnelier à front pressurisé, *Actes des Journées Nationales de Géotechnique et de Géologie de l'Ingénieur,* Grenoble, France, 779–786.

Branque, D., Subrin, D., & Boutin, D., 2002, Etude sur modèle réduit du creusement des tunnels par la méthode du bouclier à pression de terre. *Proceedings of the 3rd International Symposium on Underground Construction in soft ground, International Society for Soil Mechanics and Geotechnical Engineering,* Toulouse, France, 43–48.

Caporaletti, P., Burghignoli, A., Scarpelli, G., & Taylor, R.N. 2008. Assessment of tunnel stability in layered ground, *Geotechnical Aspects of Underground Construction in Soft Ground, Proceedings of the 6th International Symposium,* Shanghai, China, 627–633.

Doan, H.V. 2007. Creusement des tunnels en terrain meuble: étude expérimentale sur modèle réduit de tunnelier à pression de terre en sol cohérent frottant, *thèse de doctorat de l'ENTPE / INSA Lyon.*

Hagiwara, T., Grant, R.J., Calvello, M., & Taylor, R.N. 1999, The effect of overlying strata on the distribution of ground movements induced by tunneling in clay. *Soils and Foundation,* 39 (3), 63–73.

Mandel, J. 1962. Essais sur modèle réduits en mécanique des terrains. Etude des conditions de similitude, *Revue d'industrie minérale*, No. 9, 611–620.

Meguid M.A., Saada.O., Nunes M.A., & Mattar J. 2008. Physical modeling of tunnels in soft ground: A review, *Tunneling and Underground Space Technology*, n°23, pp 185–198.

Nomoto T., Imamura S., Hagiwara T., Kusakabe O., & Fujii N. 1999. Shield Tunnel Construction in Centrifuge, *Journal of geotechnical and geoenvironmental engineering*, vol 125, n°4, 289–300.

Scott, R.F. 1989. Essais en centrifugeuse et technique de la modélisation, *Revue française de géotechnique,* No. 48, 15–34.

Subrin, D., Branque, D., Berthoz, N., & Wong, H. 2009. Kinematic 3D approaches to evaluate TBM face stability: comparison with experimental laboratory observations, *Proceedings of the 2nd International Conference on computational Methods in Tunneling,* Bochum, Germany, 801–808.